Chemical Engineering Journal 158 (2010) 315–324

Contents lists available at ScienceDirect

Chemical Engineering Journal

journal homepage: www.elsevier.com/locate/cej

Chitosan based mesoporous Ti–Al binary metal oxide supported beads for defluoridation of water

Dilip Thakre [a], Sneha Jagtap [a], Nikita Sakhare [a], Nitin Labhsetwar [a], Siddharth Meshram [b], Sadhana Rayalu [a,*]

[a] National Environmental Engineering Research Institute (NEERI-CSIR), Nagpur 440020, India
[b] Department of Chemistry, Laxminarayan Institute of Technology(LIT), RTM Nagpur University, Nagpur, India

ARTICLE INFO

Article history:
Received 10 June 2009
Received in revised form
23 December 2009
Accepted 7 January 2010

Keywords:
Fluoride removal
Binary oxide
Chitosan
Adsorption isotherm
Thermodynamic parameters

ABSTRACT

In the present study, the performance of Ti–Al binary metal oxide supported beads using chitosan template was studied for fluoride removal from drinking water. The adsorbent was synthesized by precipitation method and characterized using FTIR, SEM, XRD and BET. The higher surface area of the synthesized adsorbent 323.83 m^2/g results in a much higher fluoride removal capacity Q_{max} = 2.22 mg g^{-1} as compared to bare chitosan. Pore size of beads is 42.97 Å, suggesting mesoporous nature of adsorbent. Material works very effectively at all pH except at pH greater than 9. The presence of carbonate and bicarbonate ions showed significant decline in the fluoride removal capacity of adsorbent. The experimental data fitted well to Langmuir adsorption model. The kinetic studies indicate that the system follows the pseudo-second-order and intra-particle diffusion model. Thermodynamic study reveals that the fluoride adsorption by Ti–Al binary metal oxide supported beads is an exothermic and spontaneous process. Alum appears to be the promising regeneration media showing 80% regeneration. The applicability of the adsorbent for fluoride removal was tested in field water collected from the Dhar district in Madhaya Pradesh, India.

1. Introduction

The chemical composition of water is one of the most important criteria that determine its use for a specific purpose and it varies with different sources depending on the geochemistry of that region. Fluoride is one of the most essential micronutrient present in water, which plays a dual role for human and animal health. The presence of fluoride in excess is a serious problem from a public health point of view, whereas it is beneficial when fluoride concentration is within the permissible limit of 0.5–1.5 mg L^{-1} for the prevention of tooth decay and bone formation [1]. Excessive intake of fluoride greater than the permissible limit can cause dental, skeletal and non-skeletal form of fluorosis [2,3]. Also the higher concentration of fluoride above permissible limit causes several neurological damages in severe cases [4].

The fluoride contamination of ground water widely spreads in many parts of the world and becomes a global problem. According to a UNICEFF report, millions of people are affected by fluorosis and spread in at least 25 countries across the world. In India alone, 17 states, such as Rajasthan, Madhya Pradesh, Andhra Pradesh, Tamil Nadu, Gujarat and Uttar Pradesh, are affected by higher concentration of fluoride in ground water [5]. Therefore it is necessary to bring down the fluoride concentration within the permissible limit of 0.5–1.5 mg L^{-1}.

Various treatment methods have been reported for fluoride removal from water such as precipitation [6,7], adsorption [8], ion exchange [9], electrodialysis [10], membrane process such as reverse osmosis and nanofiltration [11], and Nalgonda technique [12]. Most of the above techniques are either not very effective under the practical conditions or show limitations with respect to their implementation in rural area, cost effectiveness etc. Among these methods, adsorption is a widely used method for defluoridation of water because of its ease of operation and cost effectiveness. Development of new advanced materials for efficient and cost effective removal of fluoride from drinking water is therefore a challenging area of research and deserves immediate attention. Different adsorbents have been reported for the removal of fluoride from drinking water such as activated alumina [13], titanium rich bauxite (TRB) [14], metal oxides [15,16], clays [17–19], La(III) and Y(III) impregnated alumina [20], carbon nano tubes [21], carbon [22], alum-impregnated activated alumina [23], zeolite [24], biopolymers [25], industrial agriculture waste [26] and some other low cost materials etc [27–29].

* Corresponding author. Tel.: +91 7122247828; fax: +91 7122247828.
E-mail address: s_rayalu@neeri.res.in (S. Rayalu).

1385-8947/$ – see front matter © 2010 Published by Elsevier B.V.
doi:10.1016/j.cej.2010.01.008

Nomenclature

C_o	initial concentrations of fluoride (mg L^{-1})
C_e	equilibrium concentrations of fluoride (mg L^{-1})
h	initial sorption rate (mg g^{-1} min^{-1})
k	second order rate constant (min^{-1})
K	Langmuir constant (affinity) (L mg^{-1})
K_F	Freundlich constants related to adsorption capacity (mg g^{-1})
K_p	intra-particle diffusion rate constant (mg g^{-1} $min^{-1/2}$)
K_o	sorption equilibrium constant
n	adsorption intensity (heterogeneity factor)
q_e	equilibrium adsorbate capacity (mg g^{-1})
q_{max}	amount of adsorbate at complete monolayer coverage (mg g^{-1})
q_t	amount of fluoride adsorbed per unit mass of adsorbent at time t (mg g^{-1})
q_B	breakthrough capacity (mg g^{-1})
q_S	saturation capacity (mg g^{-1})
r	dimensionless quantity
V	volume of the aqueous solution (L)
W	mass of adsorbent (g)
ΔG°	standard free energy change (kJ mol^{-1})
ΔH°	standard enthalpy change (kJ mol^{-1})
ΔS°	standard entropy change (kJ mol^{-1})

Present study deals with the use of seafood industry waste product chitosan as template and exploring its metal binding property to incorporate Ti^{4+} and Al^{3+} ions for designing adsorbent for the defluoridation of water. Chitosan, copolymer of 2-amino-2-deoxy-D-glucopyranose and 2-acetamido-2-deoxy-D-glucopyranose, is *N*-deacetyalated product of chitin and is the second most abundant natural polysaccharide in the ecosphere after cellulose. Both chitin and chitosan are of great interest because of their unique combination of properties like biodegradability, biocompatibility and bioactivity, in addition to attractive physical and mechanical properties. It has been reported that chitosan has the highest metal coordinating ability as compared to other natural polymers. The nitrogen in the amino group of the chitosan acts as an electron donor and is presumably responsible for selective chelation with metal ion [30]. Thus, the amino and hydroxyl groups in chitosan act as the active sites for adsorption. The performance of present adsorbent for fluoride removal was also tested in the ground water obtained from Dhar District in Madhya Pradesh, India.

2. Material and methods

2.1. Materials

Chitosan was purchased from Chemchito Natural Products, Chennai, India. Ti-isopropoxide was obtained from Across organics, USA. Aluminum sulfate and all other chemicals used in this study were analytical grade obtained from E-Merck India Ltd., Mumbai, India. A stock solution of fluoride was prepared by dissolving 2.21 g Sodium fluoride in deionized water and working solution of 5 mg L^{-1} was obtained by appropriate dilution of the stock solution.

2.2. Synthesis of adsorbent

9 g of chitosan (85% deacetylated) was dissolved in 300 mL of acetic acid (CH_3COOH) solution (5% v/v) with continuous stirring by using a laboratory stirrer. In separate beakers, titanium and aluminum solution were prepared by adding 16 mL concentrated HCl to 10.69 g of Ti-isopropoxide and 11.12 g of aluminum sulfate to 25 mL distilled water respectively. Both the solutions were added to the chitosan solution and stirred for 3 h. The resulting Ti^{3+}–Al^{3+} chitosan solution was added drops wise into NH_4OH solution (50% v/v) under vigorous stirring at 250 rpm, using a syringe pump. The gel macro spheres formed were allowed to stabilize in NH_4OH solution for 1 h. The beads were separated from the NH_4OH solution and washed with deionised water. The beads were dried at 80 °C for 24 h in an oven and then calcined at 425 °C for 8 h. The calcined beads were kept in a desiccator and then allowed to cool to room temperature and washed with distilled water in 1:20 ratio and finally, dried at 80 °C for 6 h before use.

2.3. Batch adsorption study

The adsorption studies of binary metal oxide supported beads were carried out in batch process. 50 mL fluoride solution of desired concentration was taken into PVC conical flask and known weight of adsorbent was added into it and shaken for 24 h on horizontal rotary shaker (Model no. CIS-24, Remi Instruments, Mumbai, India) to attain the equilibrium. Adsorbent was then separated using Whatman filter paper no. 42 and the filtrate was analyzed for residual fluoride using Ion Selective electrode. The total ionic strength adjusting buffer (TISAB-III) was added to the samples and standard solutions in order to regulate the ionic strength of the samples and standard solutions, adjusting the pH and also to avoid the interference due to the polyvalent cations such as Al(III), Fe(III) and Si(IV). These polyvalent cations have the ability to form the complex or precipitate with the fluoride ions and reduce the free fluoride concentration in the solution. CDTA (trans-1,2-diaminocyclohexane-*N*,*N*,*N*′,*N* tetra acetic acid) form the stable complex with these polyvalent cations and form the more stable complex than the metal fluoride complex in solution. All adsorption experiments were carried out at room temperature 30 °C. The specific amount of fluoride adsorbed was calculated using following equation.

$$q_e = (C_0 - C_e) \times \frac{V}{W} \quad (1)$$

where, q_e is the adsorption amount (mg g^{-1}) in the solid at equilibrium; C_o, C_e are initial and equilibrium concentrations of fluoride (mg L^{-1}), respectively; V is volume (mL) of the aqueous solution and W is the mass (g) of adsorbent used in the experiments. The effect of pH on fluoride removal was studied by adjusting the pH of the solution using 0.1N HCl and 0.1N NaOH.

2.4. Method of analysis

After filtration, the fluoride concentration in the experimental samples was determined using fluoride ion selective electrode (Orion 9490 on a Sargent Welch pH/activity meter model PAX 900). The pH of the solution was measured using the same ion meter coupled with pH electrode. The Ti^{4+}, Al^{3+} and other heavy metals if leached from adsorbent were determined using Inductively Coupled Plasma-atomic emission spectroscopy (ICP-AES, Model OPTIMA 4100DV). Most of the experiments were repeated twice for better accuracy and blank experiments were also performed throughout the studies. Similar experimental procedure was followed for effect co-existing ions, pH and initial concentration etc.

2.5. Characterization of adsorbent

The surface morphology of the synthesized adsorbent before and after fluoride treatment was determined using Scanning Electron Microscopy (Jeol, JXA-840 A, Electron probe microanalyser, Japan). The FTIR spectra were recorded on Bruker, Model Vertex 70

spectrometer in KBr pellets. The X-ray patterns of adsorbent before and after fluoride treatment were recorded on Rigaku X-ray diffractometer. The surface area and pore size were determined using BET surface area method and BJH adsorption pore distribution.

2.6. Column experiment

Column experiment was carried out in PVC column of length 16 cm and internal diameter of 1.0 cm. The column was packed with binary metal oxide supported beads of particle size 54.42–78.71 μm and bed height was kept at 13.0 cm. Column was then fed continuously with fluoride solution of initial concentration 5 mg L^{-1} at desired flow rate using peristaltic pump (Electro Lab, Mumbai, India). The column experiments were performed at different flow rate to study its effect on fluoride adsorption capacity. The effluent samples were collected at pre-determined time intervals and analyzed for residual fluoride concentration as described in Section 2.4.

3. Result and discussion

3.1. Characterization of adsorbent

3.1.1. FTIR

The FTIR spectra of chitosan, binary metal oxide supported beads before and after calcination and after treatment with fluoride are shown in Fig. 1. The FTIR spectra of chitosan show characteristic absorption bands at 3294, 2918 and 1571 cm^{-1}, which represents –OH, $–CH_2$ aliphatic group and NH– group bending vibration respectively. The bands at 3695 cm^{-1} in chitosan can be attributed to the amino group, which is masked by the broad absorption bands from –OH group [31].

The FTIR spectra of binary metal oxide supported beads before calcinations reveals decrease in the intensity of bands at 3667, 1663 and 1571 cm^{-1}, which can be attributed to the interaction of metal ions with –NH group of chitosan molecule. The shift in the band from 1075 cm^{-1} which can be attributed to secondary –OH group to 1051 cm^{-1} suggest that the secondary hydroxyl group is coordinated with metal ions [32]. The bands at 2943 and 2881 cm^{-1} can be attributed to the $–CH_2$ and $–CH_3$ aliphatic group of polymeric backbone. The new peaks at 1356 and 1436 cm^{-1} are observed which can be assigned to C–H bending and C–N stretching vibration respectively.

The FTIR spectra of adsorbent after calcination reveal the loss of band due to $–CH_2$ and $–CH_3$ aliphatic group of polymeric backbone after calcination. The band due to –NH group is retained after calcinations at 425 °C. However, sharpening of band at 3697 cm^{-1} (–NH group), 1649, 1430 and 1365 cm^{-1} was observed after calcination, which may be due to the less intense hydrogen bonding due to the loss of broad absorption band from –OH group. The broad bands that appear in the range of 500–1000 cm^{-1} are characteristic of aluminum oxide. The broad band at 675 and 794 cm^{-1} can be assigned to bending mode of O–Al–O and Al–O stretching mode respectively [33]. The FTIR spectra of adsorbent after fluoride treatment show the shift in the band at 794 cm^{-1} to 807 cm^{-1}, indicating the interaction of fluoride with metal ions.

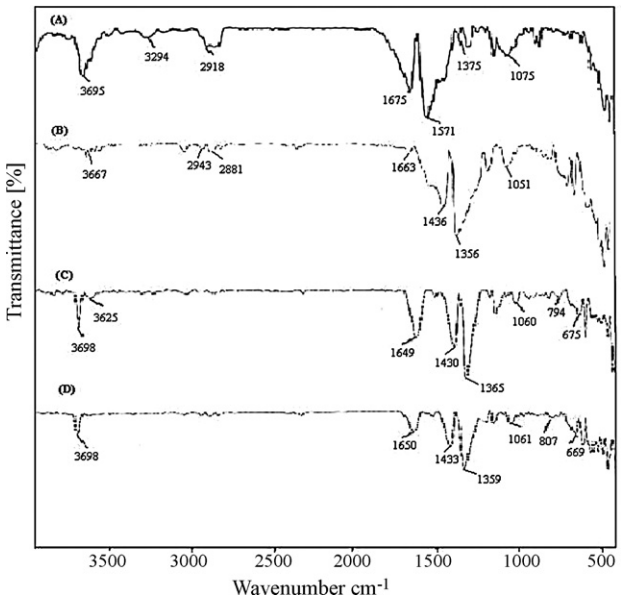

Fig. 1. FTIR spectra of (A) chitosan and (B) binary metal oxide supported beads before and after calcinations and (C) binary metal oxide supported beads after treatment with fluoride.

3.1.2. SEM

The binary metal oxide supported beads were powdered and analyzed using scanning electron microscopy and the SEM images are shown in Fig. 2. SEM image reveals not very uniform structure of binary oxide. The image reveal supported Ti–Al oxides on residual carbon from chitosan. The voids seen are due to interspaces between the chitosan fibers. The pores and voids can also be attributed to the gases liberated during the calcination and partial combustion of organic matter present. The agglomerates of

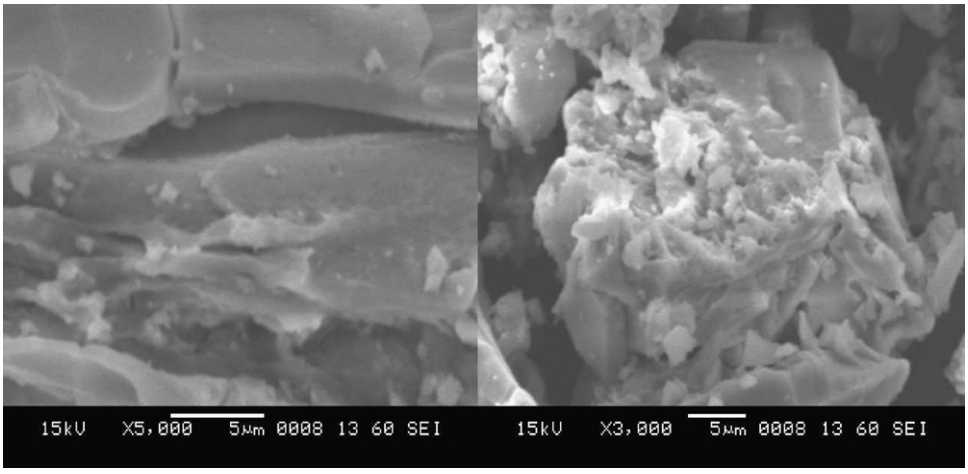

Fig. 2. SEM of binary metal oxide supported beads.

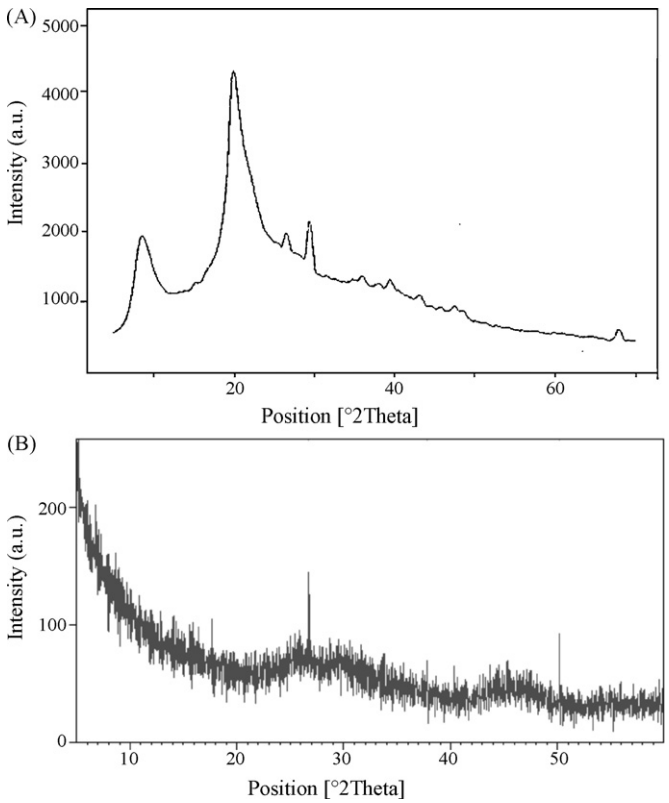

Fig. 3. XRD patterns of (a) chitosan flakes, (b) binary metal oxide supported beads.

small particles of alumina adhering over the bigger particles are observed.

3.1.3. XRD

The XRD patterns of chitosan and binary metal oxide supported beads are presented in Fig. 3. XRD pattern of chitosan show predominant crystalline peaks at 2θ values 8°, 20°, and 29°. However, these peaks are not observed for binary metal oxide supported beads. The peaks of alumina and titanium oxide are also not observed, suggesting that alumina and TiO_2 exhibits amorphous nature. The peak at 2θ value 27.6° can be assigned to the formation of aluminum titanium oxide.

3.1.4. Surface area

The most popular method used for the determination of pore size distribution is the BJH method. Pore sizes are classified into micropores (diameter (d) < 20 Å), meso-pores (20 Å < d < 500 Å) and macroporous (d > 500 Å) in accordance with the classifications adopted by International Union of Pure and Applied Chemistry (IUPAC) [34]. The surface area, pore size and pore volume of binary metal oxide supported beads were found to be 323.83 m^2/g, 42.97 Å and 0.35 cm^3/g respectively. The value of pore size suggest that binary metal oxide supported beads consist of meso-pore. The high surface area of the adsorbent can be due to well-dispersed metal oxides obtained after partial combustion of organic matter present. The results of pore size and pore volume analysis reveals the mesoporous nature of the adsorbent. The optimum size of binary metal oxide supported beads is found to be in the range of 54.42–78.71 μm.

3.2. Preliminary adsorption study

The preliminary adsorption experiments were carried out using chitosan flakes and binary metal oxide supported beads before and after calcinations at initial F^- concentration of 5.35 mg L^{-1}, contact time 24 h to check the fluoride removal efficiency of both adsorbents. The fluoride removal efficiency of these adsorbents is shown in Fig. 4a. It was observed that chitosan modified with metal oxides shows much higher fluoride removal efficiency as compare to untreated chitosan. Also, the comparison (Fig. 4a) between Ti–Al binary metal oxides supported chitosan beads before and after calcinations at 450 °C suggest that beads before calcination shows better activity for fluoride removal as compare to calcined beads. However, the uncalcined beads slightly swelled in water which leads to blockage in column and regeneration of uncalcined beads is also a problem because of the partial dissolution of beads in acidic regeneration media like alum (pH of 2% alum solution is 2.88). Therefore, the Ti–Al binary metal oxide supported chitosan beads were calcined to overcome these problems.

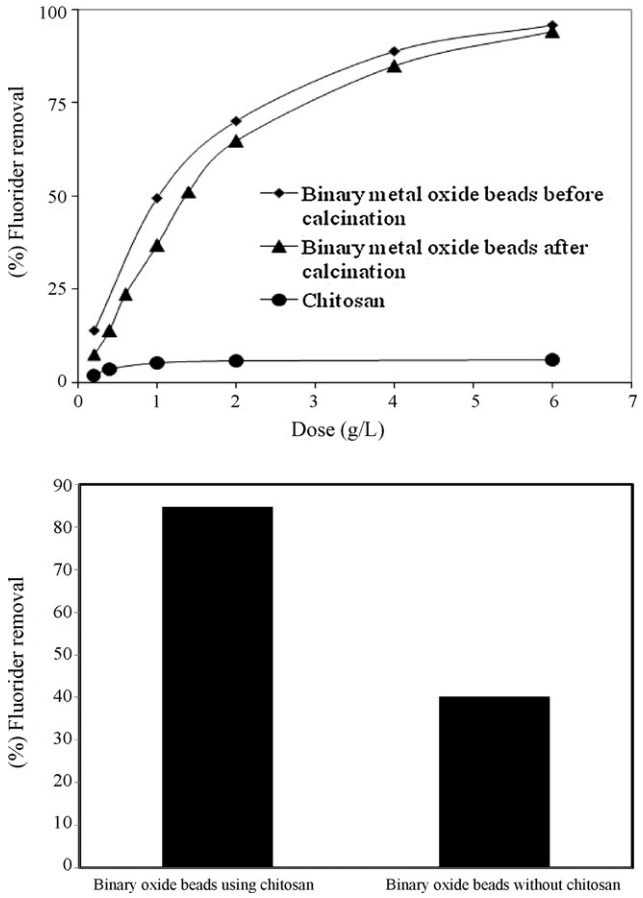

Fig. 4. Comparison of fluoride removal efficiency of (a) chitosan and binary metal oxide supported beads (b) binary metal oxide supported beads using chitosan and binary metal oxide without chitosan.

The comparison of chitosan based binary metal oxide supported beads and binary metal oxides without using chitosan was also studied at an adsorbent dose of 4 g/L for 24 h contact time and shown in Fig. 4b. It was observed that chitosan based binary metal oxide supported beads shows much better fluoride removal efficiency as compare to binary metal oxides without chitosan prepared using the similar procedure. Therefore, further adsorption studies for fluoride removal were carried out using chitosan based binary metal oxide supported beads.

3.3. Effect of adsorbent dose

The effect of adsorbent dose on fluoride removal using binary metal oxide supported beads is shown in Fig. 5. It was observed

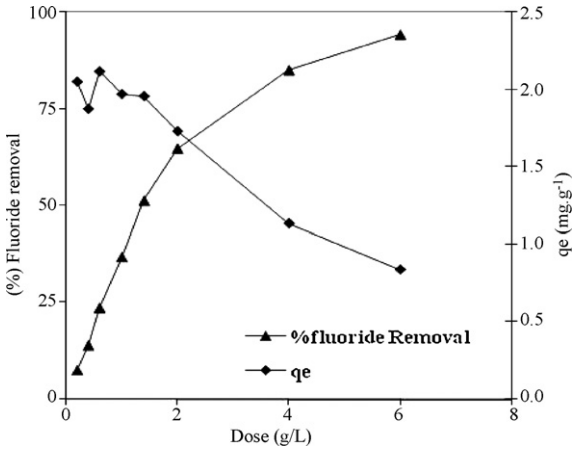

Fig. 5. Effect of dose on fluoride removal efficiency of binary metal oxide supported beads.

that percent removal of fluoride increased from 7.66–94.02% with increase in adsorbent dose from 0.2 to 6 g/L which is due to the higher active site/fluoride ratio. However, no significant change in the fluoride removal efficiency was observed after a dose of 6 g/L, which might be due to the lower equilibrium fluoride ion concentration per active site of adsorbent for adsorption. In the present study, the fluoride concentration of 0.8 mg L^{-1} was achieved at a dose of 4 g/L, which is well within the WHO guideline for fluoride in drinking water. Therefore, further studies were carried out at an adsorbent dose of 4 g/L.

3.4. Effect of initial fluoride concentration

The adsorption of fluoride on binary metal oxide supported beads was studied by varying initial fluoride concentration and keeping other parameters constant; optimum dose of 4 g/L, temperature (30 °C) and contact time of 24 h. The results are presented in Fig. 6. It was observed that with increase in initial fluoride concentration, the percent removal of fluoride decreases while the loading capacity increases. This decrease in the percent fluoride removal is due to the fact that with increase in initial fluoride concentration, the number of active sites on adsorbent surface is not enough to accommodate fluoride ions. However, at low fluoride concentration, the ratio of surface active sites to total fluoride is high and therefore fluoride ions can interact with the active sites on adsorbent surface sufficiently.

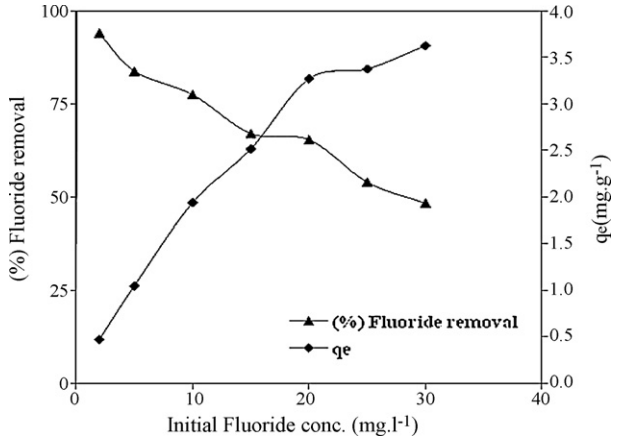

Fig. 6. Effect of initial fluoride concentration on fluoride removal efficiency of binary metal oxide supported beads.

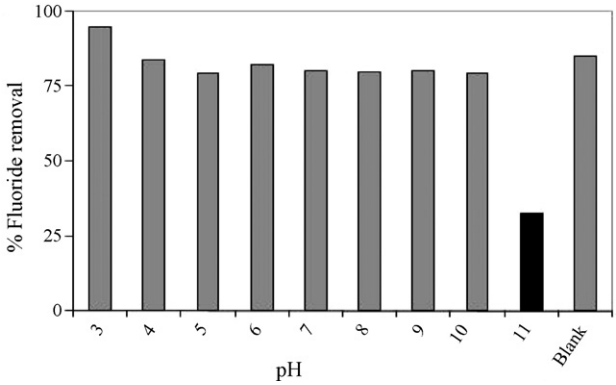

Fig. 7. Effect of pH on fluoride removal efficiency of binary metal oxide supported beads.

3.5. Effect of pH.

Behaviour of the adsorbent towards fluoride removal mainly depends on the initial solution pH. The effect of pH on fluoride removal performance of the adsorbent was studied over a wide pH range of 3–11 and the results are shown in Fig. 7. No significant change in the fluoride removal efficiency was observed over a wide pH range of 3–10. Above result can be explained by the following reaction,

$$\text{M-OH} + \text{H}^+ \Leftrightarrow \text{M-OH}_2{}^+ \quad \text{(R1)}$$

$$\text{M-OH}_2{}^+ + \text{F}^- \Leftrightarrow \text{M}^+\text{-F}^- + \text{H}_2\text{O} \quad \text{(R2)}$$

where, M represents metal ions like Al^{3+}, Ti^{3+}.

The supported titanium and aluminum oxides form the aqua complex with water and form the surface charges through amphoteric dissociation. At acidic pH, more positively charged surface sites developed which attract the negatively charged fluoride ions by electrostatic attraction resulting in the enhanced fluoride remove at acidic pH [35–37]. Reactions (R1) and (R2) hold true for fluoride adsorption at acidic medium.

$$\text{M-OH} + \text{F}^- \Leftrightarrow \text{M-F} + \text{OH}^- \quad \text{(R3)}$$

where, M represents metal ions like Al^{3+}, Ti^{3+}.

Reaction (R3) represents the ligand-exchange interaction between fluoride and hydroxyl ions at neutral pH. The increase of initial solution pH up to 10.0 has no influence on fluoride removal efficiency while further increase in pH above 10.0 drastically reduces the fluoride removal efficiency by 52%, which may be due to the competition between hydroxide and fluoride ions for active sites in this pH range. The decrease in adsorption at higher pH value (pH > 10) may also be possible due to abundance of OH^- ions which leads to increased hindrance to diffusion of fluoride ions [38]. As the fluoride removal efficiency is independent of the pH over a wide range of 3–10, these adsorbent can be used as an effective defluoridating agent over a wide pH range of 3–10.

3.6. Effect of co-existing anions

The ground water from different sources has different chemical composition depending on the minerals and geochemical deposits present in that region. Therefore, it is necessary to study the effect of co-existing ions on fluoride removal efficiency. The adsorption studies were carried out in presence of 0.01 M concentration of salt solution of sodium chloride, sodium nitrate, sodium sulfate, sodium carbonate, sodium hydrogen carbonate, sodium dihydrogen phosphate, iron sulfate and humic acid. Fig. 8 shows the effect of various ions and humic acid on fluoride removal efficiency. It was observed

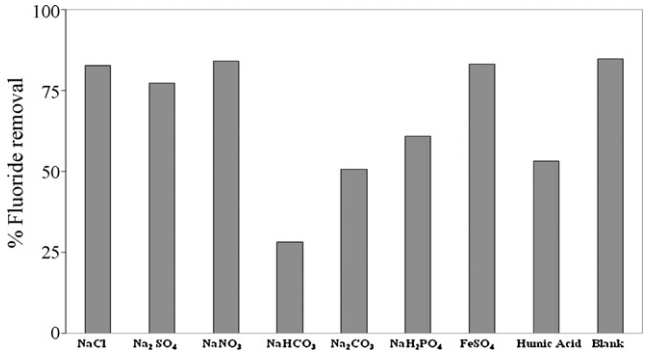

Fig. 8. Effect of co-anions on fluoride removal efficiency of binary metal oxide supported beads.

that there was no significant change in the fluoride removal efficiency in presence of chloride, nitrate and sulfate ions, whereas the presence of carbonate, bicarbonate and phosphate ions shows negative effect on the fluoride removal efficiency, which may be due to the competition of these ions with fluoride for active sites on the adsorbent [36]. The fluoride removal efficiency decreased by 24% and 34% in presence of phosphate and carbonate ions respectively, whereas it decreased by 56% in presence of bicarbonate ions. It also reveals that there was no significant change in the fluoride removal efficiency in presence of iron. However, the fluoride removal efficiency decreases significantly by 31% in presence of humic acid (0.1% solution). This decrease in fluoride removal may be due to the fact that humic acid can chelate with multivalent cations and thus decreases the availability of active sites to fluoride ions. The size of humic acid molecule also hinders the availability of the active site for fluoride resulting in decrease in fluoride removal efficiency.

4. Adsorption isotherm

The relationship between the amount of adsorbate adsorbed and its equilibrium concentration in solution can be explained by the adsorption isotherms. In order to understand the adsorption of fluoride on binary metal oxide supported beads, the experimental data was subjected to Langmuir adsorption isotherm, which is valid for monolayer adsorption on the surface of adsorbent and Freundlich adsorption isotherm, which is indicative of the surface heterogeneity of adsorbent. The linearized form of Langmuir adsorption isotherm was expressed as follows,

$$\frac{1}{q_e} = \frac{1}{q_{max}K} \times \frac{1}{C_e} + \frac{1}{q_{max}} \quad (2)$$

where, q_{max} is the amount of adsorbate at complete monolayer coverage ($mg\,g^{-1}$), which gives the maximum adsorption capacity of the adsorbent, K is the equilibrium constant of adsorbent at equilibrium which indicates the affinity of adsorbate toward adsorbent and q_e and C_e are the equilibrium adsorption capacity and equilibrium concentration of adsorbate in solution. The values of q_{max} and K were calculated from the plot of $1/C_e$ and $1/q_e$ and given in Table 1. Fig. 9a shows the plot of $1/C_e$ vs. $1/q_e$.

In order to predict the adsorption efficiency of the process, the dimensionless constant separation factor (r) was calculated by

Table 1
Langmuir and Freundlich isotherm constants for fluoride removal using binary metal oxide supported beads.

Langmuir constant			Freundlich constant		
q_{max} ($mg\,g^{-1}$)	K ($mL\,g^{-1}$)	R^2	K_F ($mg\,g^{-1}$)	$1/n$	R^2
2.22	0.11	0.96	1.40	0.10	0.94

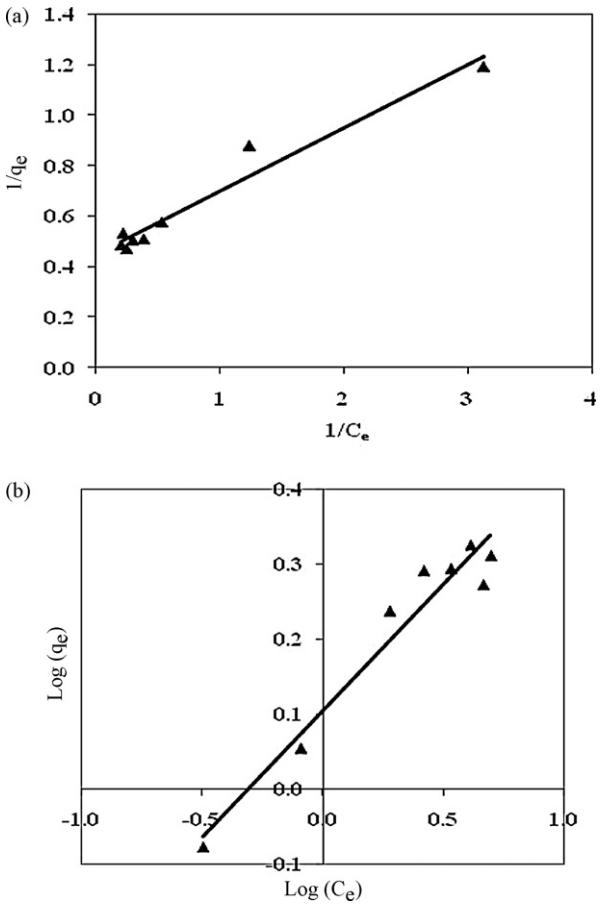

Fig. 9. (a) Langmuir and (b) Freundlich adsorption isotherm plot for fluoride removal by binary metal oxide supported beads.

using the following equation,

$$r = \frac{1}{1 + KC_o} \quad (3)$$

where, C_o and K are the initial concentration of adsobate ($mg\,L^{-1}$) and Langmuir isotherm constant. The r <1 indicate favorable adsorption and r >1 indicate unfavorable adsorption. The value of r for the initial concentration of $5.35\,mg\,L^{-1}$ was found to be 0.63. Thus it indicates that our system is favorable for adsorption.

The Freundlich model is given by the following linearized equation,

$$\log(q_e) = \log K_F + 1/n \log(C_e) \quad (4)$$

where, K_F and $1/n$ are Freundlich constants, related to adsorption capacity and adsorption intensity (heterogeneity factor) respectively. The values of K_F and $1/n$ were obtained from the slope and intercept of the linear plot of $\log(q_e)$ vs. $\log(C_e)$ and given in Table 1. Fig. 9b shows the linear plot of $\log(q_e)$ vs. $\log(C_e)$. The value of adsorption intensity $1/n$ (heterogeneity factor) is lying between 0.1 and 1.0, indicates that system is favorable for adsorption. It appears from the results that better fit was observed for Langmuir adsorption isotherm, which is also evident from the high value of R^2, which are 0.96 and 0.94 for Langmuir and Freundlich isotherms respectively. Better fit of Langmuir isotherm model indicates the monolayer uniform adsorption.

5. Adsorption kinetics

The effect of contact time on the amount of fluoride adsorbed by binary metal oxide supported beads was studied at differ-

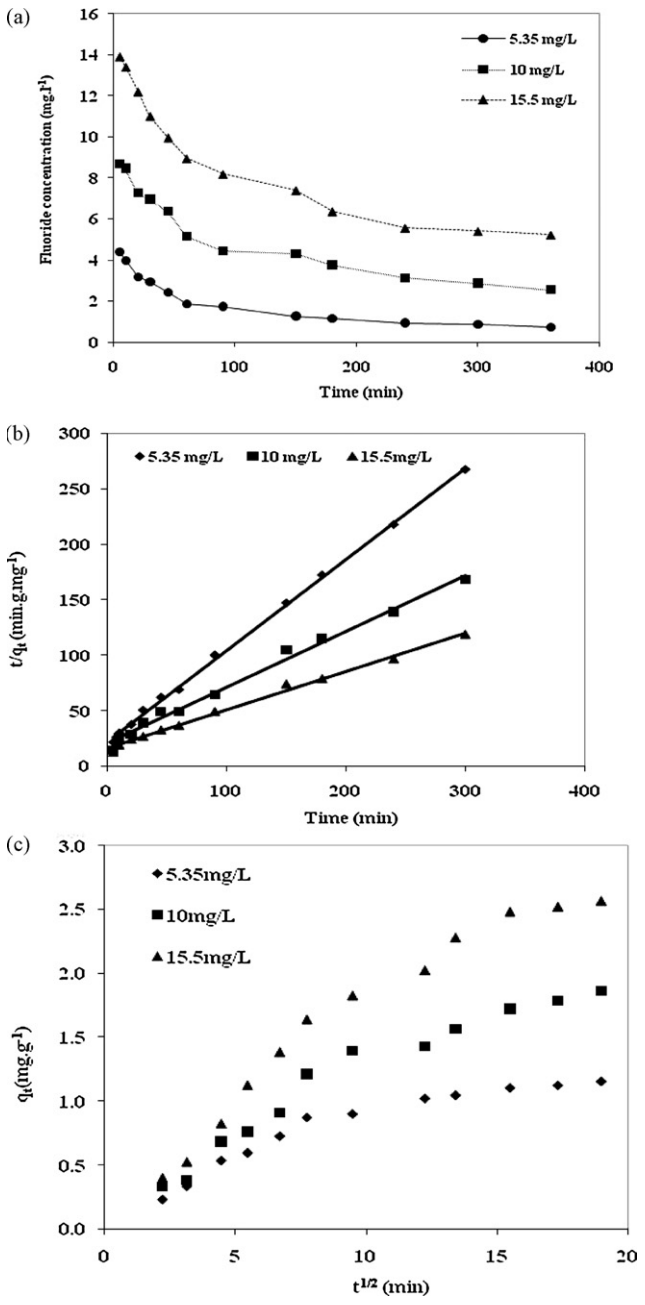

Fig. 10. (a) Effect of contact time (b) Pseudo-second-order plots and (c) Weber–Morris plots for fluoride adsorption by binary metal oxide supported beads.

ent initial fluoride concentration to determine the equilibrium adsorption time and the results are presented in Fig. 10a. It was observed that fluoride removal increases gradually with time and approaches a more or less constant value in 6 h. Various kinetic models such as reaction-based and diffusion-based models were used to understand the fluoride adsorption mechanism. The reaction-based models include pseudo-first-order and pseudo-second-order models to test the fitness of experimental data.

A pseudo-second-order chemisorption kinetic rate equation is represented as follows: [39]

$$\frac{t}{q} = \frac{1}{K_{2ads}q_e^2} + \frac{1}{q_e}t \tag{5}$$

$$h = kq_3^2 \tag{6}$$

where, q is the amount of fluoride adsorbed at time t (mg g^{-1}), q_e is the amount of fluoride adsorbed at equilibrium (mg g^{-1}), K is the second order rate constant and h is the initial sorption rate (mg g^{-1} min^{-1}). The values of q_e (1/slope), k (slope^2/intercept) and h (1/intercept) can be calculated from the plots of t/q_t vs. t and are presented in Table 2. Fig. 10b shows the plot of t/q_t vs. t. The correlation coefficient R^2 for pseudo-second-order model has higher value as compared to pseudo-first-order model indicating that the adsorption of fluoride by binary metal oxide supported beads follows second order kinetics.

To see the contribution of intra-particle diffusion on the adsorption process, the model derived by Weber and Morris was applied and is represented by the following equation:

$$q = K_p t^{0.5} \tag{7}$$

where, K_p (mg g^{-1} min$^{-1/2}$) is the intra-particle diffusion rate constant. The value of K_p can be calculated from the plot of q_t (amount of fluoride adsorbed per unit mass of adsorbent) vs. $t^{1/2}$ and are presented in Table 2. Fig. 10c shows the plot of q_t vs. $t^{1/2}$. It was observed that the plots are not linear over the whole time period and the plots exhibit dual nature with initial linear portion followed by plateau, indicating that the external surface adsorption is ruled out and the stage of intra-particle diffusion is attained and continued up to 90 min after which the equilibrium is attained. The anions are slowly transported via intra-particle diffusion into the pores of the adsorbent and finally retained in the pore. Also it was observed that the initial linear portion of the curve does not pass through the origin and latter stage of fluoride adsorption does not obey Weber–Morris equation, which indicates that mechanism of fluoride adsorption is rather complex process and the intra-particle diffusion is not the only rate-limiting step.

6. Thermodynamic parameters

In order to see the effect of temperature on adsorption of fluoride by binary metal oxide supported beads, thermodynamic parameters associated with the adsorption process, viz., standard free energy change (ΔG°), standard enthalpy change (ΔH°) and standard entropy change (ΔS°) were calculated using the following equations.

The free energy of adsorption process is represented by the equation [40]

$$\Delta G^\circ = -RT \ln K_o \tag{8}$$

where, ΔG° is the free energy of sorption (kJ mol^{-1}), T is the temperature in Kelvin, R is the universal gas constant (8.314 J mol^{-1} K^{-1}) and K_o is the sorption equilibrium constant. The sorption equilibrium constant K_o for the sorption reaction was determined from the

Table 2
Pseudo-second-order kinetic and intra-particle pore diffusion model parameters for binary metal oxide supported beads.

C_o (mg L^{-1})	Pseudo-second-order parameters				Intra-particle pore diffusion model	
	q_e (mg g^{-1})	k (g mg^{-1} min^{-1})	h (mg g^{-1} min^{-1})	R^2	K_p (mg g^{-1} min$^{-1/2}$)	R^2
5.35 (~5)	1.22	0.031	0.045	0.99	0.052	0.94
10.0(~10)	1.98	0.012	0.048	0.99	0.092	0.94
15.5(~15)	2.87	0.008	0.062	0.99	0.13	0.88

Table 3
Thermodynamic parameters for fluoride adsorption by binary metal oxide supported beads.

T (K)	K_o	ΔG° (kJ mol^{-1})	ΔH° (kJ mol^{-1})	ΔS° (kJ mol^{-1} K^{-1})
303	7.73	−5.15	−0.50	0.015
313	7.69	−5.31		
323	7.63	−5.46		

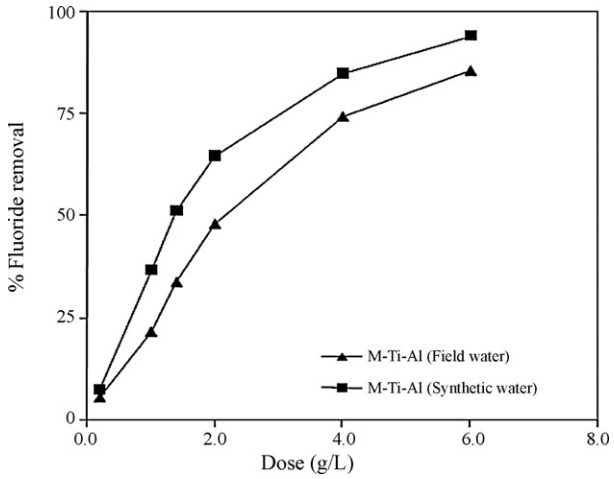

Fig. 11. Comparison of fluoride removal efficiency of binary metal oxide supported beads in synthetic and field water.

slope of the plot of ln (q_e/C_e) vs. C_e at different temperatures and extrapolating to zero C_e according to method suggested by Khan and Singh [41].

The sorption equilibrium constant K_o may be expressed in terms of enthalpy change (ΔH°) and entropy change (ΔS°) as a function of temperature and is shown below.

$$\ln K_o = \frac{\Delta H^\circ}{RT} + \frac{\Delta S^\circ}{RT} \quad (9)$$

where, ΔH° is the heat of sorption (kJ mol^{-1}) and ΔS° is the standard entropy change (kJ mol^{-1} K^{-1}). The values of ΔH° and ΔS° can be obtained from the slope and intercept of a plot of ln (K_o) vs. $1/T$. The values of K_o, ΔG°, ΔH° and ΔS° are presented in Table 3. The negative values of ΔG° and positive value ΔS° suggests that fluoride adsorption by binary metal oxide a supported bead is feasible and spontaneous in nature. Also the negative value of ΔH° suggests that the process of fluoride adsorption is exothermic in nature.

7. Field trial

The applicability of the adsorbent for the removal of fluoride from natural water sample collected from tube wells at fluoride-affected area in Dhar, Madhaya pradesh, India is shown in Fig. 11. The detailed characteristic parameters of field water before and after treatment are given in Table 4. It was observed that the fluoride adsorption capacity of the adsorbent decreases from 2.22 mg g^{-1} in simulated water to 1.71 mg g^{-1} in the natural water sample collected from field. This decrease in the adsorp-

Table 4
Detailed characteristics of field water before and after treatment.

Parameters	Before treatment	After treatment
Turbidity (NTU)	2	3
pH	8.10	8.26
TDS (mg L^{-1})	237	256
Conductivity (μS cm^{-1})	245	264
Alkalinity (mg L^{-1})	116	117
Total hardness (mg L^{-1})	100	118
Fluoride (mg L^{-1})	5.35	1.37
Cl$^-$ (mg L^{-1})	14	16
SO_4^- (mg L^{-1})	11.78	22.85
Nitrate (mg L^{-1})	<0.01	<0.01
Aluminium (mg L^{-1})	<0.002	0.025
Titanium (mg L^{-1})	<0.001	<0.001

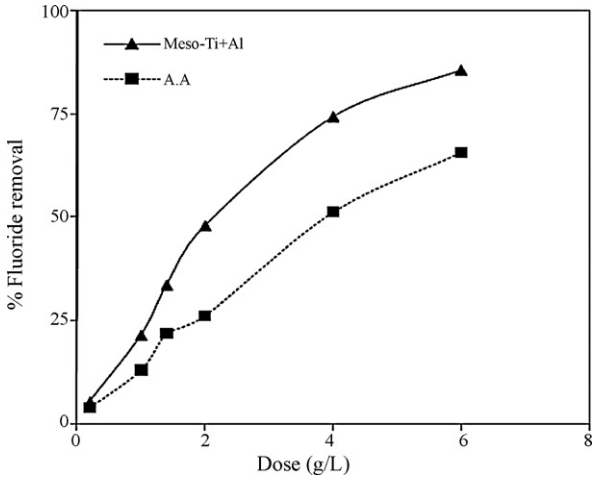

Fig. 12. Comparison of fluoride removal efficiency of binary metal oxide supported beads and activated alumina.

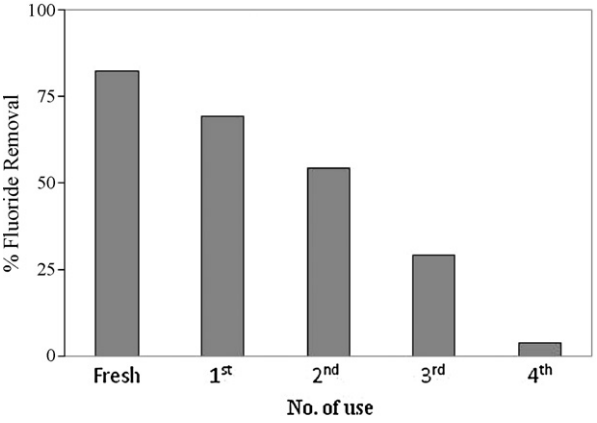

Fig. 13. Reuse study of binary metal oxide supported beads.

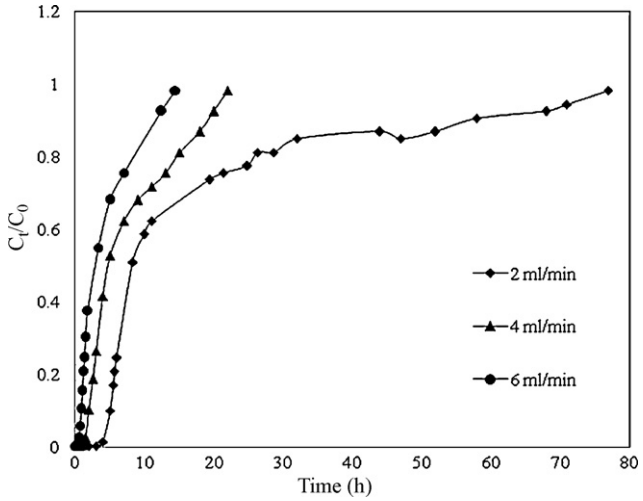

Fig. 14. Plot of C_t/C_o vs. time at different flow rate.

Table 5
Breakthrough and saturation capacity of binary metal oxide supported beads at different flow rates.

Flow rate (mL min^{-1})	EBCT (min)	Breakthrough time (min)	Breakthrough capacity (q_B) (mg g^{-1})	Saturation capacity (q_S) (mg g^{-1})
2	5	340	0.43	1.34
4	2.6	150	0.37	1.14
6	1.3	70	0.26	0.88

tion capacity could be due to the presence of different cations and anions of the field water. A marginal increase in the pH after treatment with adsorbent was observed which suggest the ligand-exchange mechanism between fluoride and hydroxyl ions. The fluoride removal efficiency of binary metal oxide supported beads was also compared with the conventional adsorbent activated alumina and shown in the Fig. 12. It was observed that the synthesized adsorbent has higher fluoride removal efficiency as compare to conventional adsorbent activated alumina. It was reported in literature that activated alumina has certain limitation for fluoride removal from water such as higher dose, pH dependent and the presence of co-ions greatly affect the fluoride removal efficiency [13]. In our case also the lesser fluoride removal efficiency of activated alumina was observed which might be due to the higher pH of field water. Also, negligible leaching of aluminium and titanium ions was observed from the adsorbent.

8. Reuse and regeneration of adsorbent

The reusability of the adsorbent was studied in order to check the residual fluoride uptake capacity. The reusability experiment was carried out by repeating the adsorption experiment on used and oven dried sample under similar condition used for the first cycle and is shown in Fig. 13. It was observed that the used adsorbent still have significant fluoride uptake capacity. The 1st and 2nd reuse shows decrease of fluoride removal efficiency by 13% and 28% respectively, while 3rd reuse shows decrease of 53%. This indicates that the adsorbent does not exhaust its fluoride uptake capacity in one cycle and oven drying of the used sample results in significant fluoride adsorption in subsequent cycles. After complete saturation adsorbent was subjected to regeneration using different regeneration media like sodium hydroxide, alum and ammonium chloride. 0.5 g of fluoride loaded material was shaken with 50 mL of regeneration media for 1 h on a horizontal rotary shaker. Adsorbent was separated by filtration and washed with deionized water and dried at 80 °C for 4 h. Regenerated adsorbent was subjected for fluoride adsorption experiment to determine the fluoride removal efficiency.

It was observed that multiple treatments with alum solution appear to be the promising regeneration media and a maximum of 80% regeneration was achieved with 2% alum solution.

9. Column experiment

The effect of flow rate on fluoride adsorption capacity of binary metal oxide supported beads was studied at a flow rate of 2, 4 and 6 mL/min. Fig. 14 shows the plot of C_t/C_o vs. time at different flow rate. It is observed that at a lower flow rate of 2 mL/min, fluoride removal was efficient at least in the initial stage of process, which may be due to the adequate contact time between adsorbent and adsorbate in solution. However, the extent of fluoride removal decreases with gradual occupancy of active sites of adsorbent. Removal of fluoride ions at slower rate continues after the breakthrough point. At higher flow rate, the breakthrough time and fluoride removal capacity decreases and breakthrough becomes steeper. This decrease in breakthrough time and fluoride removal capacity is due to shorter residence time of solute in the column, because of which, fluoride solution elutes the column before fluoride adsorption equilibrium occurs. The values of breakthrough capacity (q_B) and saturation capacity (q_S) of binary metal oxide supported beads at different flow rate are given in Table 5. The maximum breakthrough and saturation capacities were observed at a flow rate of 2 mL/min.

10. Conclusion

In the present study, various experiments were carried out to study the performance of binary metal oxide supported beads for fluoride removal from water. Thermodynamic study reveals that the fluoride adsorption by binary metal oxide supported beads is feasible and spontaneous in nature. Synthesized adsorbent shows excellent defluoridation capacity of q_{max} = 2.22 mg g^{-1} with negligible release of aluminium and titanium ions. The binary metal oxide beads works very efficiently over a wide pH range of 3–9. No significant change in the fluoride removal capacity was observed in the presence of co-anions such as chloride, nitrate and sulfate except for carbonate and bicarbonate ions. Kinetic study reveals that the system follows pseudo-second-order kinetic and mechanism of fluoride adsorption is rather complex process and the intra-particle diffusion is not the only rate-limiting step. The equilibrium data agree well with Langmuir adsorption isotherm. The characterization results revel that the material exhibit high surface area and is mesoporous in nature. It is possible to regenerate the adsorbent by giving multiple treatments with alum. No significant change was observed in the chemical composition of field water after treatment with adsorbent and no leaching of metal was also observed. The column study reveals the efficient fluoride adsorption at lower flow rate. The chemical parameters of water are well within the permissible limit.

Acknowledgements

We thankfully acknowledge to Council of Scientific and Industrial Research (CSIR) for granting the fellowship as two of the authors Mr. Dilip Thakre and Ms. Sneha Jagtap are CSIR senior research fellows and constant support & guidance of Dr. T. Chakrabarty, Director NEERI. Financial assistance from, UNICEF Bhopal, India for this work is gratefully acknowledged.

References

[1] WHO (World Health Organization), Fluorine and Fluorides, Environmental Health Criteria, Geneva, (1984) 36.
[2] S. Ayoob, A.K. Gupta, Fluoride in drinking water: a review on the status and stress effects, Crit. Rev. Environ. Sci. Technol. 36 (2006) 433–487.
[3] R.C. Meenakshi, Maheshwari, Fluoride in drinking water and its removal, J. Hazard. Mater. 137 (2006) 456–463.
[4] A.K. Susheela, Treatise on Fluorosis, Fluorosis Research and Rural Development Foundation, India, 2001.
[5] S.M. Maliyekkal, A.K. Sharma, L. Philip, Manganese-oxide-coated alumina: a promising sorbent for defluoridation of water, Water Res. 40 (2006) 3497–3506.
[6] A.K. Yadav, C.P. Kaushik, A.K. Haritash, A. Kansal, R. Neetu, Defluoridation of groundwater using brick powder as an adsorbent, J. Hazard. Mater. 128 (2006) 289–293.
[7] H. Mjengera, G. Mkongo, Appropriate defluoridation technology for use in fluorotic areas in Tanzania, Phys. Chem. Earth 28 (2003) 1097–1104.
[8] X. Wu, Y. Zhang, X. Dou, M. Yang, Fluoride removal performance of a novel Fe–Al–Ce trimetal oxide adsorbent, Chemosphere 69 (2007) 1758–1764.

[9] N.I. Chubar, V.F. Samanidou, V.S. Kouts, G.G. Gallios, V.A. Kanibolotsky, V.V. Strelko, I.Z. Zhuravlev, Adsorption of fluoride, chloride, bromide and bromate ions on a novel ion exchanger, J. Colloid Interface Sci 291 (2005) 67–74.
[10] S. Annouar, M. Mountadar, A. Soufiane, A. Elmidaoui, M.A. Menkouchi Sahli, Defluoridation of underground water by adsorption, on the chitosan and by electrodialysis, Desalination 165 (2004) 437–438.
[11] A. Lhassani, M. Rumeau, D. Benjelloun, M. Pontie, Selective demineralization of water by nanofiltration application to the defluoridation of brackish water, Water Res. 35 (2001) 3260–3264.
[12] W.G. Nawlakhe, D.N. Kulkarni, B.N. Pathak, K.R. Bulusu, Defluoridation of water by Nalgonda technique, Indian J. Environ. Health 17 (1975) 26–65.
[13] S. Ghorai, K.K. Pant, Equilibrium, kinetics and breakthrough studies for adsorption of fluoride on activated alumina, Sep. Purif. Technol. 42 (2005) 265–271.
[14] N. Das, P. Pattanaik, R. Das, Defluoridation of drinking water using activated titanium rich bauxite, J. Colloid Interface Sci. 292 (2005) 1–10.
[15] B. Nagappa, G.T. Chandrappa, Mesoporous nanocrystalline magnesium oxide for environmental remediation, Microporous Mesoporous Mater. 106 (2007) 212–218.
[16] D. Mohapatra, D. Mishra, S.P. Mishra, G.R. Chaudhary, R.P. Das, Use of oxide minerals to abate fluoride from water, J. Colloid Interface Sci. 275 (2004) 355.
[17] A. Tor, Removal of fluoride from an aqueous solution by using montmorillonite, Desalination 201 (2006) 267–276.
[18] P.P. Coetzee, L.L. Coetzee, R. Pukal, S. Mubenga, Characterization of selected South African clays for defluoridation of natural waters, Water SA. 29 (2003) 331–338.
[19] S. Kagne, S. Jagtap, P. Dhawade, S.P. Kamble, S. Devotta, S.S. Rayalu, Hydrated cement: a promising adsorbent for the removal of fluoride from aqueous solution, J. Hazard. Mater. 154 (2008) 88–95.
[20] S.A. Wasay, S. Tokunaga, S.W. Park, Removal of hazardous anions from aqueous solution by La(III)-and Y(III)- impregnated alumina, Sep. Sci. Technol. 31 (1996) 1501–1514.
[21] Y.-H. Li, S. Wang, X. Zhang, J. Wei, C. Xu, Z. Luan, D. Wu, Adsorption of fluoride from water by aligned carbon nanotubes, Mater. Res. Bull. 38 (2003) 469–476.
[22] R.L. Ramos, J. Ovalle-Turrubiartes, M.A. Sanchez-Castillo, Adsorption of fluoride from aqueous solution on aluminum impregnated carbon, Carbon 37 (1999) 609–617.
[23] S.S. Tripathy, J.-L. Bersillon, K. Gopal, Removal of fluoride from drinking water by adsorption onto alum-impregnated activated alumina, Sep. Purif. Technol. 50 (2006) 310–317.
[24] M.S. Onyango, Y. Kojima, O. Aoyi, E.C. Bernardo, H. Matsuda, Adsorption equilibrium modeling and solution chemistry dependence of fluoride removal from water by trivalent-cation-exchanged zeolite F-9, J. Colloid Interface Sci. 279 (2004) 341–350.
[25] W. Ma, Y. Fei-Qun, M. Han, R. Wang, Characteristics of equilibrium, kinetics studies for adsorption of fluoride on magnetic-chitosan particle, J. Hazard. Mater. 143 (2007) 296–302.
[26] S. Chidambaram, A.L. Ramanathan, S. Vasudevan, Fluoride removal studies in water using natural materials, Water SA. 29 (2003) 339–344.
[27] E. Oguz, Adsorption of fluoride on gas concrete materials, J. Hazard. Mater. B 117 (2005) 227–233.
[28] M. Mahramlioglu, I. kizilicikii, I.O. Bicer, Adsorption of fluoride from aqueous solution by acid treated spent bleaching earth, J. Fluorine Chem. 115 (2002) 41–47.
[29] W.H. Kang, E.I. Kim, J.Y. Park, Fluoride removal capacity of cement paste, Desalination 202 (2007) 38–44.
[30] W.S. Wan, S. Ngah, A. Ghani, A. Kamari, Adsorption behaviour of Fe(II) and Fe(III) ions in aqueous solution on chitosan and cross-linked chitosan beads, Bioresour. Technol. 96 (2005) 443–450.
[31] A.T. Pauline, J.I. Simionato, J.C. Garcia, J. Nozaki, Characterization of chitosan and chitin produced from silkworm chrysalides, Carbohydr. Polym. 64 (2006) 98–103.
[32] A.J. Varma, S.V. Deshpande, J.F. Kennedy, Metal complexation by chitosan and its derivative: a review, Carbohydr. Polym. 55 (2004) 77–93.
[33] A.R. Choudhuri, C.G. Takoudis, Investigation of the aluminum oxide/Si (1 0 0) interface formed by chemical vapor deposition, Thin Solid Films 446 (2004) 155–159.
[34] V.C. Srivastava, I.D. Mall, I.M. Mishra, Characterization of mesoporous rice husk ash (RHA) and adsorption kinetics of metal ions from aqueous solution onto RHA, J. Hazard. Mater. B134 (2006) 257–267.
[35] S. Ayoob, A.K. Gupta, P.B. Bhakat, V.T. Bhat, Investigation on the kinetics and mechanisms of sorptive removal of fluoride from water using alumina cement granule, Chem. Eng. J. 140 (2008) 6–14.
[36] S. Kamble, S. Jagtap, N. Labhsetwar, D. Thakre, S. Godfrey, S. Devotta, S.S. Rayalu, Defluoridation of drinking water using chitin, chitosan and lanthanum-modified chitosan, Chem. Eng. J. 129 (2007) 173–180.
[37] M. Sarkar, A. Banerjee, P.P. Pramanick, A.R. Sarkar, Use of laterite for the removal of fluoride from contaminated drinking water, J. Colloid Interface Sci. 302 (2006) 432–441.
[38] A.R. Tembhurkar, S. Dongre, Studies on fluoride removal using adsorption process, J. Environ. Sci. Eng. 48 (2006) 151–156.
[39] S. Meenakshi, N. Viswanathan, Identification of selective ion exchange resin for fluoride sorption, J. Colloid Interface Sci. 308 (2007) 438–450.
[40] S. Meenakshi, C. Sairam Sundaram, R. Sukumar, Enhanced fluoride sorption by mechanochemically activated kaolinites, J. Hazard. Mater. 153 (2008) 164–172.
[41] A.A. Khan, R.P. Singh, Adsorption thermodynamics of carbofuran on Sn(IV) arsenosilicate in H^+, Na^+ and Ca^{2+} forms, Colloids Surf. 24 (1987) 33–42.